Propistsova *et al. EvoDevo (2025) 16:2*
https://doi.org/10.1186/s13227-025-00238-6

EvoDevo

RESEARCH

Open Access

Shedding light on the embryogenesis and eye development of the troglophile cave spider *Tegenaria pagana* C. L. Koch, 1840 (Araneae: Agelenidae)

Evgenia A. Propistsova[1,2*], Guilherme Gainett[3,4], Ariel D. Chipman[1,2], Prashant P. Sharma[5,6] and Efrat Gavish-Regev[2]

Abstract

Background Relatively little is known about the diversity of embryonic development across lineages of spiders, even though the study of embryonic development is a primary step in evo-devo studies and essential for understanding phenotypic evolution. Practically nothing is known about embryogenesis in cave-dwelling spiders, animals which play an important role in cave ecosystems and may have remarkable adaptations to aphotic habitats such as loss of eyes.

Results Here, we describe embryogenesis and study the expression patterns of several genes of the Retinal Determination Network (RDN) in the troglophile (species that have pre-adaptations to life in caves, and can complete their life cycle in caves, as well as in epigean habitats) eye-bearing funnel-web spider species *Tegenaria pagana* C. L. Koch, 1840, using fluorescent staining and confocal microscopy. We discuss the characteristic features of *T. pagana* embryogenesis and key RDN genes. Although in many respects the embryonic development of different species of entelegyne spiders is similar, we found differences in the rate of development, and the details of the opisthosoma, respiratory system, and brain morphogenesis in comparison with established spider model species. Our data supports the hypothesis of a conserved role of *sine oculis* gene in the eye formation of arachnids.

Conclusions Given the recent discovery of congeneric cave species with different degrees of eye reduction throughout Israel, these data sets provide a foundational point of comparison for studying eye reduction and eye loss events in the spider genus *Tegenaria*.

Keywords Funnel-web Spiders, Development, Eyes, Cave fauna

*Correspondence:
Evgenia A. Propistsova
evgeniia.propistsova@mail.huji.ac.il
Full list of author information is available at the end of the article

Background

Caves and other subterranean environments represent ecologically distinct ecosystems with unique abiotic conditions [7, 16]. Environmental conditions such as the absence of direct sunlight, constant temperatures, relatively high humidity, and reduced or no local primary production [31] may lead cave-dwelling species to undergo various behavioral, morphological, and physiological adaptations. Cave-dwelling species may present troglomorphic traits, such as reduction or loss of eyes due to the absence of light, depigmentation, and attenuated bodies or appendages [15, 16, 43]. With the reduction of eyes, cave-dwelling species often develop heightened non-visual senses, including proprio- and chemoreception [45]. Troglomorphic traits, including eye reduction, have been studied extensively in the Mexican tetra blind cave fish *Astyanax mexicanus* (De Filippi, 1853), (Characiformes, Characidae) [13, 30, 33] and the cave isopod *Asellus aquaticus* (Linnaeus, 1758) (Isopoda, Asellidae) [34, 42]. However, there is a lack of comparative data on other elements of cave fauna that exhibit the classical troglomorphic phenotype, such as arachnids, which play an important role as predators in cave ecosystems [24]. Spiders have attracted attention in the context of comparative development due to a different number and arrangement of eyes in comparison with better-studied arthropods [8, 26], as well as because of a whole genome duplication event that is thought to have impacted their evolution and phenotype [38].

More than 52,000 species of spiders have been described [47]. Complete embryonic development (from fertilization to hatching) has been documented for only three species: *Cupiennius salei* Keyserling, 1877 (Trechaleidae) [46], *Parasteatoda tepidariorum* (C. L. Koch, 1841) (Theridiidae) [25], and *Acanthoscurria geniculata* (C. L. Koch, 1841) (Theraphosidae) [28]. The staging system for embryogenesis varies from 14 stages in *P. tepidariorum*, and *A. geniculata* to 21 stages in *C. salei*, and designation of stages largely draws upon the leading spider model, *P. tepidariorum* (Fig. 1). A handful of studies has addressed differences in embryonic development between mygalomorph, Synspermiata and entelegyne spiders [28, 40, 44] such as the morphogenesis of a tube-like opisthosoma in basally branching spiders and differences in the number of book lungs and spinnerets after embryogenesis. However, these studies were not focused on describing the complete process of embryogenesis, making it difficult to compare data between those few species [2, 23, 29, 40, 44, 48]. In addition, there are no data on the embryogenesis of cave dwelling spiders, which could help in the study of their evolution and development.

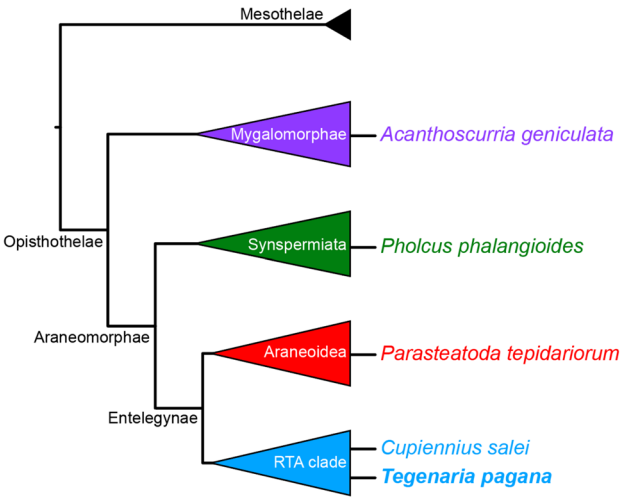

Fig. 1 Simplified tree of Araneae indicating the key species discussed in this paper. Topology based on Kulkarni et al. [20]

The funnel-web genus *Tegenaria* Latreille, 1804 (Araneae, Agelenidae) currently includes 135 species, with eleven species inhabiting caves in Israel [47]. Cave-dwelling *Tegenaria* species present a gradient of eye reduction, from a complete loss to fully developed eyes [1]. The incidence of a spectrum of eye phenotypes within a single genus offers a potentially powerful system for understanding how modifications of gene regulatory networks incur an array of morphological phenotypes in cave habitats. The Retinal Determination Network of genes (hereafter RDN) is a complex and highly regulated molecular network that controls the process of retinal development in various vertebrate and invertebrate animal eyes [22, 27]. This network consists of several associated genes mostly encoding transcription factors that together determine the fate of cells of the eye retina and other eye structures. Research on the genes of the RDN in spiders has mainly relied on comparative analysis with other arthropods, such as insects and crustaceans [27]. These studies revealed conserved key genes and pathways involved in retinal determination across diverse phyla [3]. In the fruit fly *Drosophila melanogaster* Meigen, 1830, an iconic system for understanding eye development, two *Pax6* homologs (*eyeless* and *twin of eyeless*) are responsible for the initiation of eye formation. *Pax6* activates the expression of a set of downstream genes, including *eyes absent* (*eya*), *sine oculis* (*so*), and *dachshund* (*dac*), which form a "gene regulatory network" to control cell proliferation and differentiation [22]. In spiders, duplicates of many of these genes have been shown to be transcriptionally active, dissimilar in expression patterns between gene copies, and variable across species. The role of *Pax6* genes in spider eye development is still not

well understood and the expression of *Pax6* genes varies in different spider species. While two *Pax6* orthologs were isolated from *P. tepidariorum* spiders [38], they are not expressed in any of the eyes but in the neurogenic ectoderm. However, *Pax6* is expressed in the ocular segment of *Parasteatoda* in early germ band stages, which could be the upstream signal that primes the expression of *eya*/*so* into what is interpreted as the eye progenitor cells in later stages [9]. There is also no eye-specific *Pax6* expression in five other spider species recently surveyed [12]. However, in *C. salei* [36] one *Pax6* homolog is expressed in the principal eyes but not in the secondary eyes. *Pax6* expression has not been found in the developing eyes of the chelicerate horseshoe crab *Limulus polyphemus* (Linnaeus, 1758) [5], despite its expression in their lateral sense organ, a sensory structure whose function remains unresolved. It is possible that an alternative mechanism may exist for the initiation of eye development in this case. Notably, both *eyeless* and *twin of eyeless* are indeed expressed in the developing eyes of the harvestman *Phalangium opilio* Linnaeus, 1758, and particularly in the lentigenic cells, though their function has not been explored [11]. The lack of expression of *Pax6* in eyes of most spider species suggests that alternative pathways may exist in these species for eye development, and more research is needed to better understand the role of *Pax6* orthologs in spider eye development.

Recent advances in comparative data sets across spiders offer new directions for understanding the ontogeny of troglomorphism in arachnids, with an emphasis on eye reduction. As a first step, we describe here the complete embryonic development and key Retinal Determination Network genes expression in the troglophile eye-bearing spider species *Tegenaria pagana* C. L. Koch, 1840. We also develop a methodology for maintaining a laboratory culture of *T. pagana* for developmental study.

Results

1. *Tegenaria pagana* embryonic development

We provide a general overview table containing lateral views of DAPI stained embryos at all stages alongside corresponding schematic images (Fig. 2).

Stage 1 (0–10 h after eggs laying (hAEL)). Early cleavages. Eggs of *T. pagana* are spherical with a diameter of 500–600 µm. Eggs are mostly composed of yolk, which is present as fine homogeneous granules. The nuclear divisions and yolk cleavage take place intralecithally (deep within the yolk) inside the egg (Figs. 2, st. 1; 3, st. 1) as in *P. tepidariorum* [25]. In the first hours, we expect the nuclei to be surrounded by a mass of yolk and not yet enclosed within cell membranes as in *P. tepidariorum* [25]. During these cleavages, energids (nuclei and their surrounding plasma) migrate to the surface of the egg (Fig. 3, st. 1c, d).

Stage 2 (11–30 hAEL). Blastoderm. Early cleavages are followed by nuclear mitosis and the formation of the blastoderm (Figs. 2, st. 2; 3, st. 2). All cleavage energids reach the surface. Blastodermal cells have an irregular polygonal shape with a large nucleus in the middle (Fig. 3e st. 2). The blastodermal cells become more rounded after a few cleavage cycles. At later stages after 2–3 h, some energids are located slightly lower than others (white arrows at Fig. 3e and g st. 2). As proposed in a study of *C. salei* [46] these might be vitellophages or just some of the cells left in the yolk after migration.

Stage 3 (31–49 hAEL). Blastopore formation. Over the following few hours (Figs. 2, st. 3; 3, st. 3), most of the blastodermal cells start to shift (indicated by arrows in Fig. 3i, st.3) and gradually gather in a particular region of the blastoderm. These cells begin aggregating to form the blastopore. There is no formation of a distinct germ disc (a dense aggregation of cells that provides the primordial tissue for the embryo body and is found in some arthropod embryos). This is unlike in *P. tepidariorum* [25], where there is a clearly outlined germ disc but similar to *C. salei* [46]. At this stage most cell divisions are asynchronous (Suppl. 1). A small number of cells aggregate at the center of the forming germ disc and begin the formation of the blastopore (Bp) (Fig. 3i, st. 3). In contrast with the other studied species, the blastopore of *T. pagana* can be seen indistinctly in confocal scans as a small depression in the cell mass.

Stage 4 (50–72 hAEL). Primary thickening. Blastopore cells begin to ingress beneath the blastoderm (internalization) and initiate gastrulation (Figs. 2, st. 4; 3, st. 4). In the opposite hemisphere of the egg the blastoderm cells are evenly distributed, although there are fewer of them. During this process, the blastopore rises slightly above the surface of the embryo and is visible as a protrusion (Fig. 3k, st. 4). At the end of stage 4, the blastopore closes, losing the elevation. That suggests the end of gastrulation at this site and the primary thickening formation (PT, an agglomerate of the first internalizing cells at the center of the blastopore [14]) at the blastopore region (Fig. 3j, st. 4).

Stage 5 (73–106 hAEL). Cumulus migration. Mesendodermal cells at this stage form two groups of cells in the primary thickening region. A larger group of cells that separates from the center of the primary thickening and is visible as a slight elevation above the surface of the embryo (cumulus, Cu) (Figs. 2, st. 5; 3, st. 5) migrates in an arc toward the second half of the embryo at approximately 100–110 degrees. Once the other hemisphere of the embryo is reached, the cumulus starts to disappear

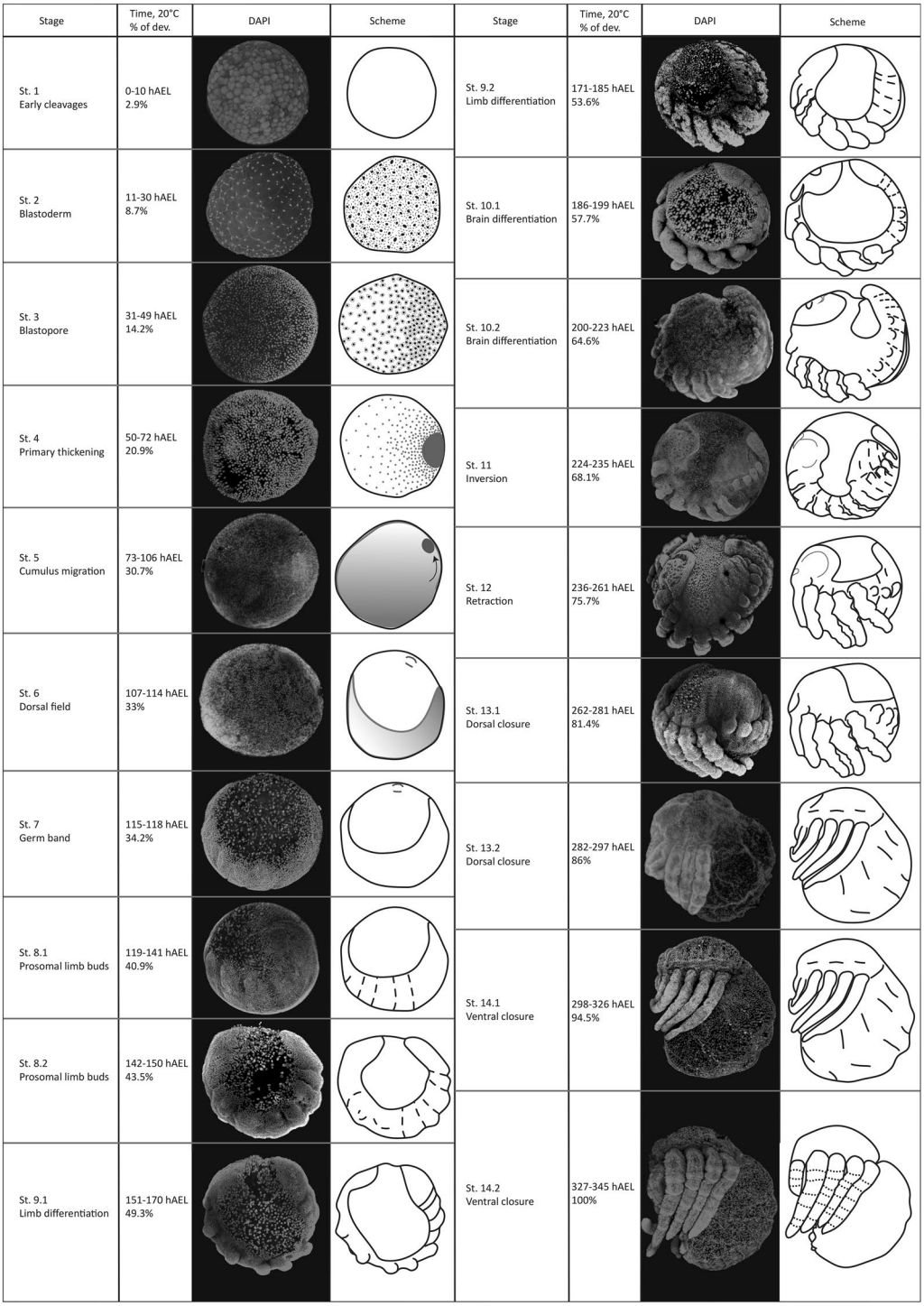

Fig. 2 Overview of the embryonic development of *T. pagana*. Embryos in lateral view, timing with percent of the development, and embryo schematic drawings. DAPI staining, embryonic stages 1 to 14.2. Black dots on st. 2, 3 and 4 indicate blastoderm nuclei and the dotted line in st. 2 indicates blastoderm cell outlines. Black arrow indicates cumulus migration. Less cell dense region at st. 5 and 6 is displayed in white, cell dense region in grey. The dorsal field at st. 6 is indicated by the cumulus silhouette

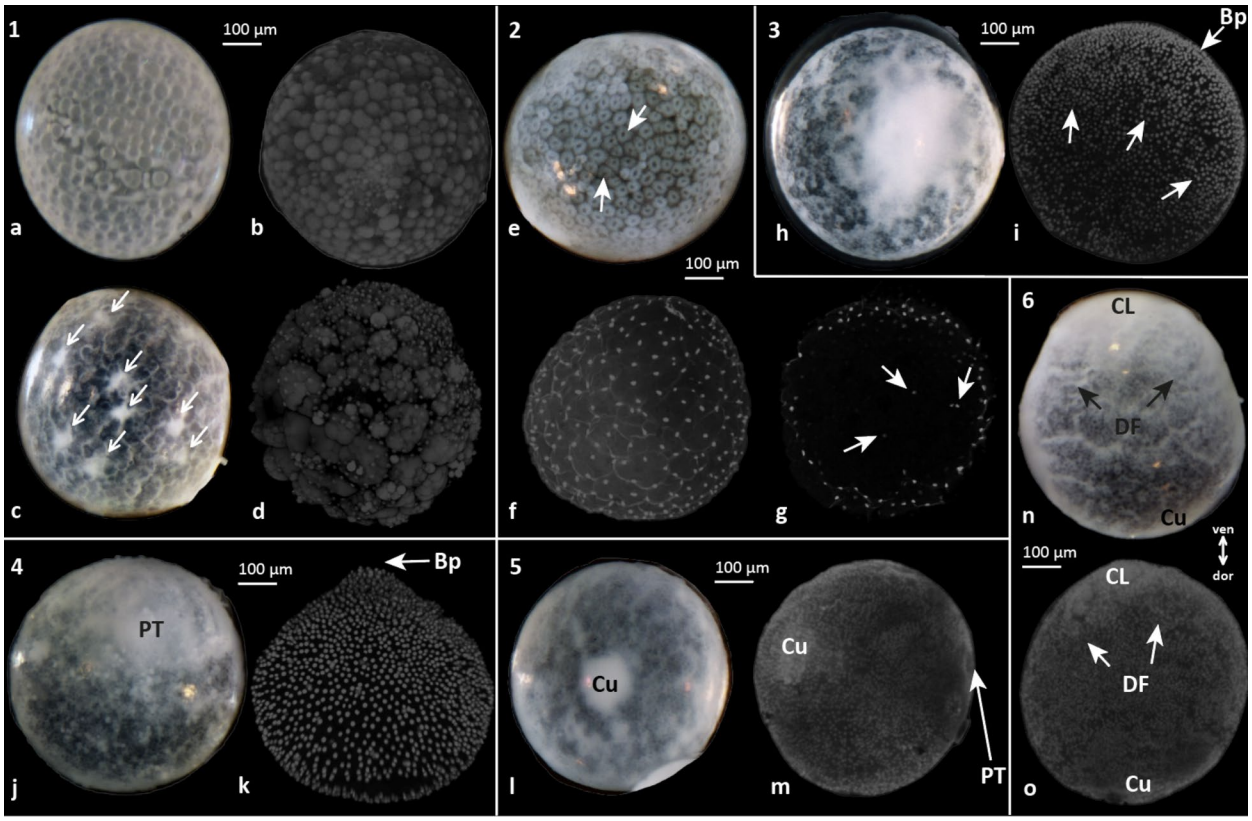

Fig. 3 Stages 1–6 of embryonic development of *T. pagana*. Light microscopy (*a*, *c*, *e*, *j*, *l*, *n*) and DAPI staining (*b*, *d*, *f*, *h*, *i*, *k*, *m*, *o*) of different embryos. The numbers in each panel represent the different embryonic stages. Bp: blastopore; CL: caudal lobe; Cu: cumulus; DF: dorsal field; PT: primary thickening. *c*, white arrows indicate nuclei. *e*, white arrows indicate energids that are located slightly lower than others. *h*, *n*, *o* arrows indicate cell migration

marking the dorsal pole of the embryo. A second smaller group of cells remains in the center of the embryonic portion of the egg and continues to be identified as the primary thickening (PT) indicating the posterior pole (Fig. 3m, st. 5). During the movement of the cumulus, some of the cells gather around the primary thickening, and another part migrates radially from the primary thickening. As in the previously studied *C. salei* [46] and *P. tepidariorum* [25] embryos, *T. pagana* embryos have a less transparent pole (where the mesendoderm is concentrated) and a more transparent one with the yolk.

Stage 6 (107–114 hAEL). Dorsal field. During this stage, cells from the primary thickening begin to migrate in the direction opposite to the cumulus and laterally, forming a zone with less densely packed cells, called the dorsal field (DF) (Figs. 2, st. 6 and 3, st. 6). Toward the end of this stage, the cumulus finally disappears and an elevation of tissue forms in place of the primary thickening, which will later become the posterior end of the embryo (the caudal lobe, CL).

Stage 7 (115–118 hAEL). Germ band. The process of lateral extension of the dorsal field continues. A C-shaped germ band (a ventral strip of embryonic cells with a convex flexion, bearing the caudal lobe at its posterior end) appears at the ventral side (Fig. 2, st. 7). Compared to the dorsal field, it has a significantly higher cell density. The germ band expands over the entire ventral pole. Its posterior region is now called the segment addition zone (SAZ) (Fig. 4, st. 7). Only the prosomal segments are determined by this stage.

Stage 8 (119–150 hAEL). Prosomal limb buds. At stage 8.1, the significantly expanded germ band occupies about 300 degrees of the egg perimeter (Figs. 2, st. 8.1 and 4, st. 8.1). The SAZ has a higher cellular density than the anterior portion, which is called the precheliceral region (Pc). The precheliceral region is broader than the rest of the germ band (Fig. 4e, st. 8.1). Between the precheliceral region and the SAZ, six segments become evident, marking the future chelicerae (Ch), pedipalps (P), and walking legs (L1–4). The ocular segment is presumably included within the precheliceral region.

At stage 8.2 the germ band extends anteriorly and posteriorly, bringing the precheliceral region and SAZ closer together (Figs. 2, st. 8.2 and 4, st. 8.2). The cell density

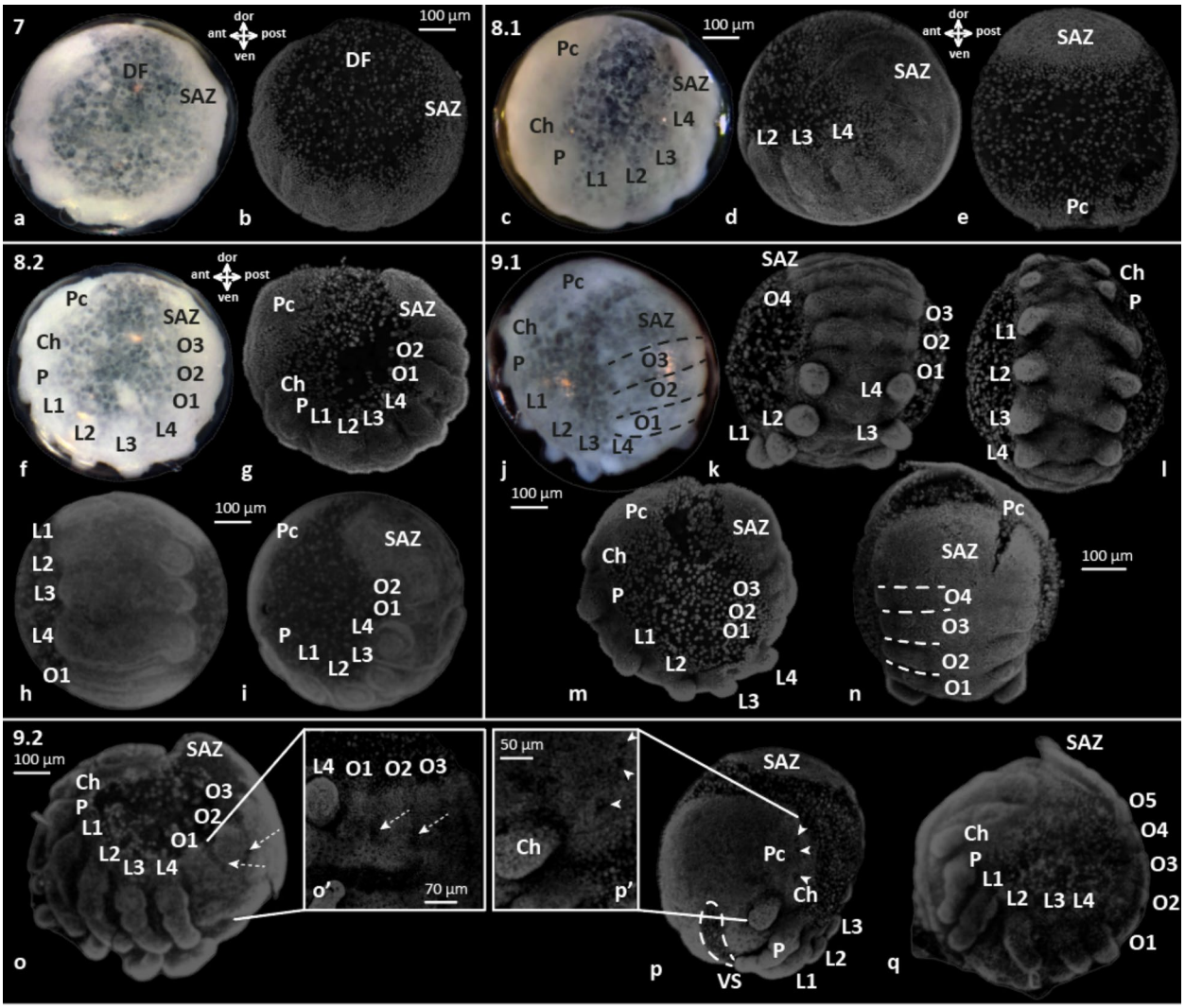

Fig. 4 Stages 7–9.2 of embryonic development of *T. pagana*. Light microscopy (*a*, *c*, *f*, *j*) and DAPI staining (*b*, *d*, *e*, *g–i*, *k–r*). The numbers in each panel represent the different embryonic stages. Ch: chelicera; DF: dorsal field; L1–4: walking legs; O1–5: opisthosomal segments; P: pedipalp; Pc: precheliceral region; SAZ: segment addition zone; VS: ventral sulcus (also marked by dotted line). *o*, dotted line arrow indicates book lung system formation; *p*, white arrowheads mark point-like depressions of internalized neural precursor cells

in the SAZ increases. The prosomal segments become more distinct. The appendage buds of all prosomal segments (chelicera, pedipalps, and four walking legs) begin to grow. The first three opisthosomal segments (O1–3) are also formed, much more demarcated than in previously studied species [25, 46]. In contrast to *C. salei* [46] and *P. tepidariorum* [25] during this stage it is not possible to clearly see the ventral sulcus (a thin layer of tissue between the germ band halves).

Stage 9 (151–185 hAEL). Limb differentiation. Stage 9.1 is characterized by prosomal limb bud elongation and bulging outward. Cheliceral buds are slightly smaller than the leg buds. The precheliceral region and segment addition zone grow closer to each other, more similar to *P. tepidariorum* [25] than *C. salei* [46] (Figs. 2, st. 9.1 and 4, st. 9.1). None of the prosomal limb buds are segmented yet, and they may in some cases develop asymmetrically left–right turning into normal embryos afterward (Fig. 4l, st. 9.1). The number of growing opisthosomal segments increases to four. All opisthosomal segments are roughly the same size, unlike in *P. tepidariorum.*

At stage 9.2 (Fig. 4, st. 9.2) many structures that appear in the early stages of *P. tepidariorum* [25] develop. At this stage, the developing book lung system becomes visible (Fig. 4o, st. 9.2, dotted line arrow) and point-like depressions of internalized neural precursor cells in the

precheliceral region (Pc) (Figs. 2, st. 9.2 and 4p, st. 9.2, white arrowheads). The ventral sulcus (VS) becomes noticeable at this stage unlike in *C. salei* [46] and *P. tepidariorum* [25], where it happens earlier. SAZ elongates and almost touches the precheliceral lobe (Fig. 4o, p, st. 9.2) as in *P. tepidariorum* [25], and unlike *C. salei* [46]. The precheliceral region have several depressions of neuronal precursor groups (Fig. 4p, st. 9.2). The prosomal appendages elongate, and the tips converge toward each other. The segments of the walking legs become increasingly visible as development proceeds (Fig. 4o, q, st. 9.2). The number of opisthosomal segments increases to five.

Stage 10 (186–223 hAEL). Brain differentiation. At stage 10.1 (Figs. 2, st. 10 and 5, st. 10.1) the precheliceral region develops, and neural development leading to distinct furrows and folds in the brain region proceeds. Now the precheliceral region (Pc) is separated into bilateral precheliceral lobes (PcL). Laterally on each precheliceral lobe, a lateral furrow, a kidney-shaped area sunk into the tissue (dotted line on Fig. 5b, st. 10.1) appears. The stomodeum (Sto) develops as a new structure (Fig. 5b, st. 10.1). Above it, a paired labrum (Lb) is formed. Endites at the pedipalp coxae become visible. The tips of forming walking legs are now touching each other. Opisthosomal limb buds (LB), all about the same size, are now evident on segments O1–O5. Unlike in *P. tepidariorum* [25], where opisthosomal limb buds 3–4 are larger than the first and second. In addition, the number of opisthosomal segments in *T. pagana* increases up to six, whereas in *P. tepidariorum* [25], their number increases to nine, and in *C. salei* [46] up to eight at a corresponding stage based on bilateral precheliceral lobes separation. The ventral sulcus (VS) expands to the fifth opisthosomal segment (Fig. 5c, st. 10.1). Precheliceral lobes and SAZ are still close to each other and more similar to *P. tepidariorum* [25] than to *C. salei* [46].

Stage 10.2 (Fig. 5, st. 10.2) is characterized by brain development: the medial subdivisions (ms) in the upper brain parts and the lateral subdivisions (ls) in the sides of the brain are developing. In late stages, an anterior furrow (AF) appears above medial subdivisions; these furrows form a semi-crescent from the labrum to the lateral furrow (LF) and show a high density of neuronal point-like depressions (Fig. 5e, st. 10.2). The two distal lobes of the labrum are clearly visible. The walking legs are now clearly separated into five limb segments by annulations. The number of opisthosomal segments increases to seven. Opisthosomal buds 4 and 5 are now bigger than the second and third. In the precheliceral area, as well as in the opisthosoma, numerous point-like depressions of neural precursors are evident. The ventral sulcus is growing to the segment addition zone.

Stage 11 (224–235 hAEL). Inversion. At this stage, the yolk is internalized as the opisthosomal segments grow laterally (Figs. 2, st. 11; 5, st. 11). The segment addition zone now protrudes slightly from the yolk, marking the start of the tail-like formation of the 'post-opisthosoma', while lateral parts of the opisthosomal segments are growing in anterodorsal direction (white arrows on Fig. 5g, st. 11). The number of opisthosomal segments is now ten with four opisthosomal buds on segments O2–O5. In the brain region, the medial and lateral subdivisions expand anteriorly and partly overgrow anterior and lateral furrows (Fig. 5h, st. 11). The anterior furrow grows medially and reaches the labrum at later stages. The two labral buds are fused medially. The chelicerae are divided into two segments: base (bs) and fang (f), which is a bit later than in *P. tepidariorum* [25], where it happens at stage 10.2. The pedipalps now have four segments with endites on the coxa. The walking legs are now separated into six segments. A cell accumulation underneath the transverse slit at the posterior edge of opisthosomal segment 2 is visible due to the development of the book lung system (dotted line arrows on Fig. 5i, i', st. 11). The ventral sulcus expands laterally and shortens reaching opisthosomal segment 4 unlike in *P. tepidariorum* [25] or *C. salei* [46].

Stage 12 (236–261 hAEL). Retraction. At this stage, a significant change in the shape of the entire embryo occurs, because of considerable retraction of the germ band, meaning that the posterior end veers away from the precheliceral lobe (Figs. 2, st. 12 and 5, st. 12). As a result of this movement, the distance between the precheliceral region and the posterior opisthosomal region increases (Fig. 5k, st. 12). At the same time, internalization of the yolk continues by the tergal (Ter) plates of the

(See figure on next page.)

Fig. 5 Stages 10.1–14.2 of embryonic development of *T. pagana*. DAPI staining. The numbers in each panel represent the different embryonic stages. AF: anterior furrow; ASp: anterior spinneret; AT: anal tubercle; B: brain; bs: base; Ch: chelicera; cx: coxa; en: endite; f: fang; fe: femur; H: heart; L1–4: walking legs; Lb: labrum; LB: limb bud; LF: lateral furrow; ls: lateral subdivision; ms: medial subdivision; MSp: median spinneret; mt: metatarsus; O1–5: opisthosomal segments; P: pedipalp; pa: patella; PcL: precheliceral lobe; PS: prosomal shield; PSp: posterior spinneret; SAZ: segment addition zone; Sp: spinneret; Sto: stomodeum; T: tail; ta: tarsus; Ter: tergite; ti: tibia; tr: trochanter; VS: ventral sulcus. *b*, arrowheads indicate neural precursor tissue, dotted line indicates lateral furrow; *c*, dotted line indicates ventral sulcus; *d*, *h*, dotted line separate leg segments; *g*, *l*, arrows indicate tissue movement; *i*, *k*, *m*, *n*, dotted line arrow indicates book lung system formation; *n*, white arrow indicates the egg teeth; *o*, dotted line indicates remains of the anterior furrow; *o*, *r*, *x*, red arrowheads indicate secondary eyes, yellow arrowhead indicates principal eyes zone

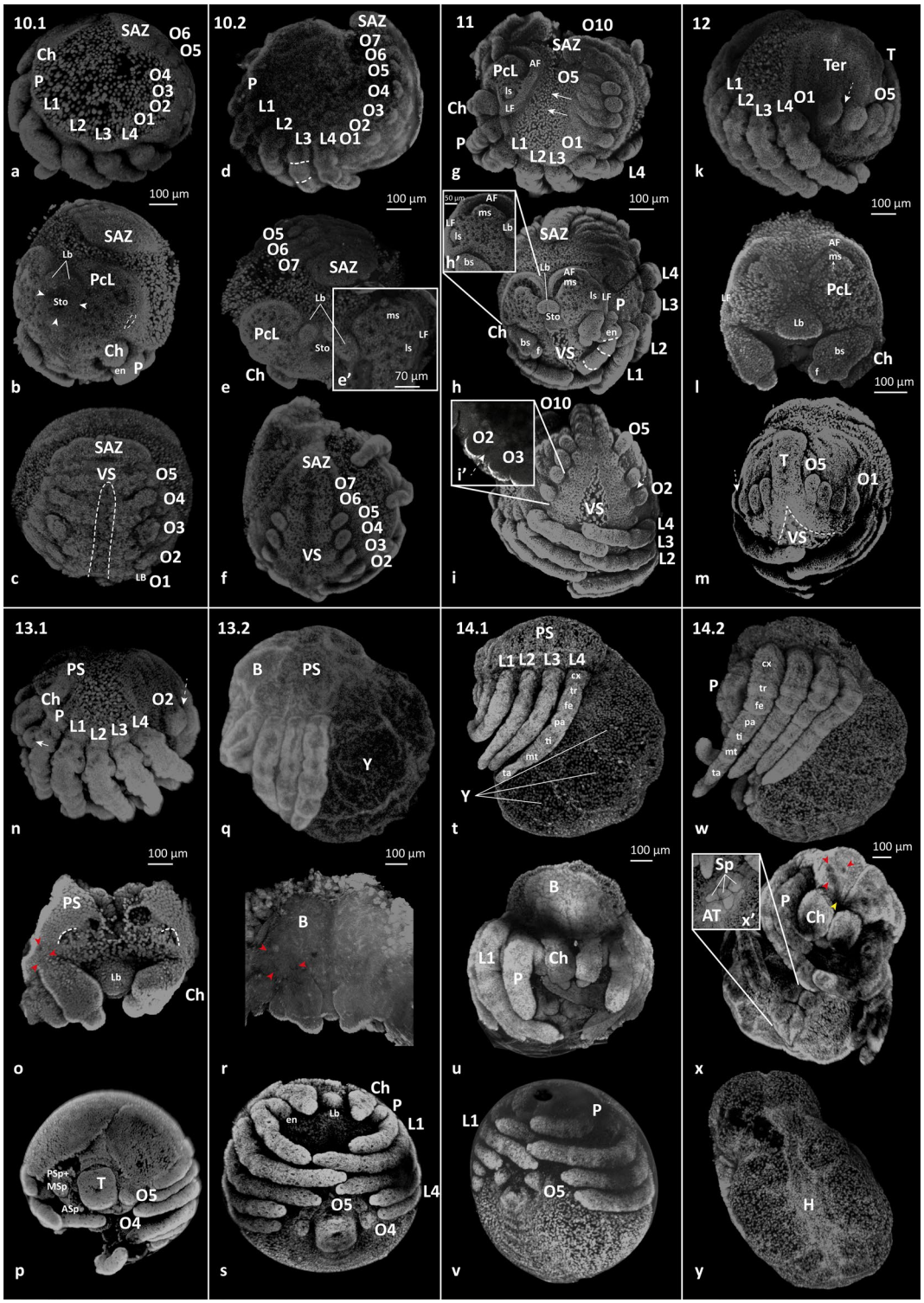

Fig. 5 (See legend on previous page.)

prosoma and opisthosoma. The lateral furrows of the developing brain are almost covered by the expansion of the lateral subdivisions, while the anterior furrows start to close by the anterior expansions of the medial subdivisions. The two halves of the brain start to approach medially. The labrum and mouth area migrate posteriorly and

are now situated at the same level as the anterior edge of the chelicerae. The tip of the labrum is stretched medially and points in a ventral direction. The labrum increases slightly in size compared to the previous stage. The walking legs are arranged in a zipper-like manner and are now separated into seven segments by annulations. The ventral sulcus expands laterally but remains at the level of the opisthosomal segments 4–5 unlike in *P. tepidariorum* [25] or *C. salei* [46], where it splits up to segments 8–9. The process of growth of the ventral sulcus in *T. pagana* is more similar to that of *P. tepidariorum* [25]. The ventral sulcus does not grow as strongly laterally as in *C. salei* [46]. The appendages of the opisthosomal segments remain undifferentiated, with the fourth pair of appendages (the nascent anterior spinnerets) still larger than the others and opisthosomal segment five, the nascent posterior/medial spinnerets, continue to elongate and achieve a bulb-like shape. Opisthosomal segments 6–10 form a structure called the tail (T).

Stage 13 (262–297 hAEL). Dorsal closure. At stage 13.1 the tergites of both body halves finally connect dorsally, starting from the most posterior tergites of the caudal region toward the anterior direction initiating the dorsal closure of the embryo (Figs. 2, st. 13.1 and 5, st. 13.1). Closure happens earlier in the opisthosomal region, while the later closure of the prosoma forms the prosomal shield (PS). The tissue of the precheliceral lobes grows toward the labrum and covers the brain, leaving only remains of the anterior furrow. For the first time, three pairs of developing secondary eyes can be detected above the chelicerae (red arrowheads on Fig. 5o, st. 13.1). The labrum has moved posteriorly and is now situated more or less between the chelicerae. The egg teeth develop on the most proximal segment of the pedipalps. Opisthosomal buds become oval. The posterior sides of the limb buds on opisthosomal segment 2 become concave, and the longitudinal opening of the pulmonary sac becomes broader. During the process of the differentiation of anterior (ASp), posterior (PSp) and medial spinnerets (MSp), opisthosomal buds four and five move under the embryo body and show slight annulations. The tail moves under the body of the embryo, while the dorsal closure happens (Fig. 5p, st. 13.1).

At stage 13.2 cuticle covers the whole brain (B) and expands all over the dorsal prosomal area nearly completing a prosomal shield (Figs. 2, st. 13.2 and 5, st. 13.2). Secondary eyes move apart and develop above the chelicerae. The labrum migrates further posteriorly and is situated behind the chelicerae. In the frontal view, the chelicerae partly cover the labrum. The yolk now occupies almost all the opisthosomal volume and is divided into three cellular sac-like yolk compartments. While the petiolus (the narrow connection between the prosoma and opisthosoma) starts to narrow, the yolk migrates from prosoma to opisthosoma. This movement leads to a change of the embryo form, from oval to buckled. The opisthosomal sternites during this stage converge medially from the posterior end anteriorly, starting with the spinneret-bearing segments O4 and O5.

Stage 14 (298–345 hAEL). Ventral closure. Stage 14.1 is characterized by the final formation of the prosomal shield (Figs. 2, st. 14.1 and 5, st. 14.1). The walking legs show their final segmentation (Fig. 5t, st. 14.1). In frontal view, the labrum is completely covered by the chelicerae (Fig. 5u, st. 14.1). The future petiolus continues to narrow. It is now about 60% of the width of the prosoma. The spinneret-bearing opisthosomal segments migrate medially and the posterior opisthosomal segments become more compressed.

At stage 14.2, the final stage in this scheme, the cuticle completely develops (Figs. 2, st. 14.2 and 5, st. 14.2). The heart is fully visible in the dorsal side of the opisthosoma (Fig. 5y, st. 14.2). The petiolus is narrowing to its final width separating prosoma and opisthosoma. The cheliceral bases become wider and the fangs of the chelicerae become tapered and start to point at each other. Secondary eyes are arranged as a triangle on each side and the principal eyes are evident medially above the chelicerae (Fig. 5x, st. 14.2, red arrowheads indicate secondary eyes, yellow arrowhead indicates principal eyes). Due to the proceeding unfolding process, the anal tubercle and the spinning field become visible. Spinnerets are now fully developed with the posterior spinnerets longer than the anterior ones, which is typical for the entire Agelenidae.

2. Key retinal determination genes (RDGs) expression in developing *Tegenaria pagana* eyes

To understand the primary pattern of eye formation in *T. pagana* embryogenesis, we surveyed genes that were reliably found to be involved in eye development in other studied species [4, 27, 36]. We were unable to find *Pax6* in the transcriptome data, so the expression of this gene was not included here. We included *Pax2.1* (*sv*, *shaven* in *Drosophila*) in this study, since a recent study suggests that it is a promising candidate for inducing spider lateral eye development [17] but see [11] We examined the expression of a total of eight genes: *Pax2.1*, *sine oculis 1* (*so1*), *eyes absent* (*eya*), *orthodenticle 2* (*otd2*), *dachshund 1* (*dac1*), *dachshund 2* (*dac2*), *Six3.2*, and *atonal 1* (*ato1*) for stages 9.2–14 (Fig. 6).

Pax2.1: We detected the expression of *Pax2.1* as small round regions above the chelicerae, in the region of the secondary eye formation (Fig. 6, *Pax2.1*). At stage 9.2 it is almost undetectable, while at stage 10.1 the signal becomes much stronger. At late stage 14 *Pax2.1*

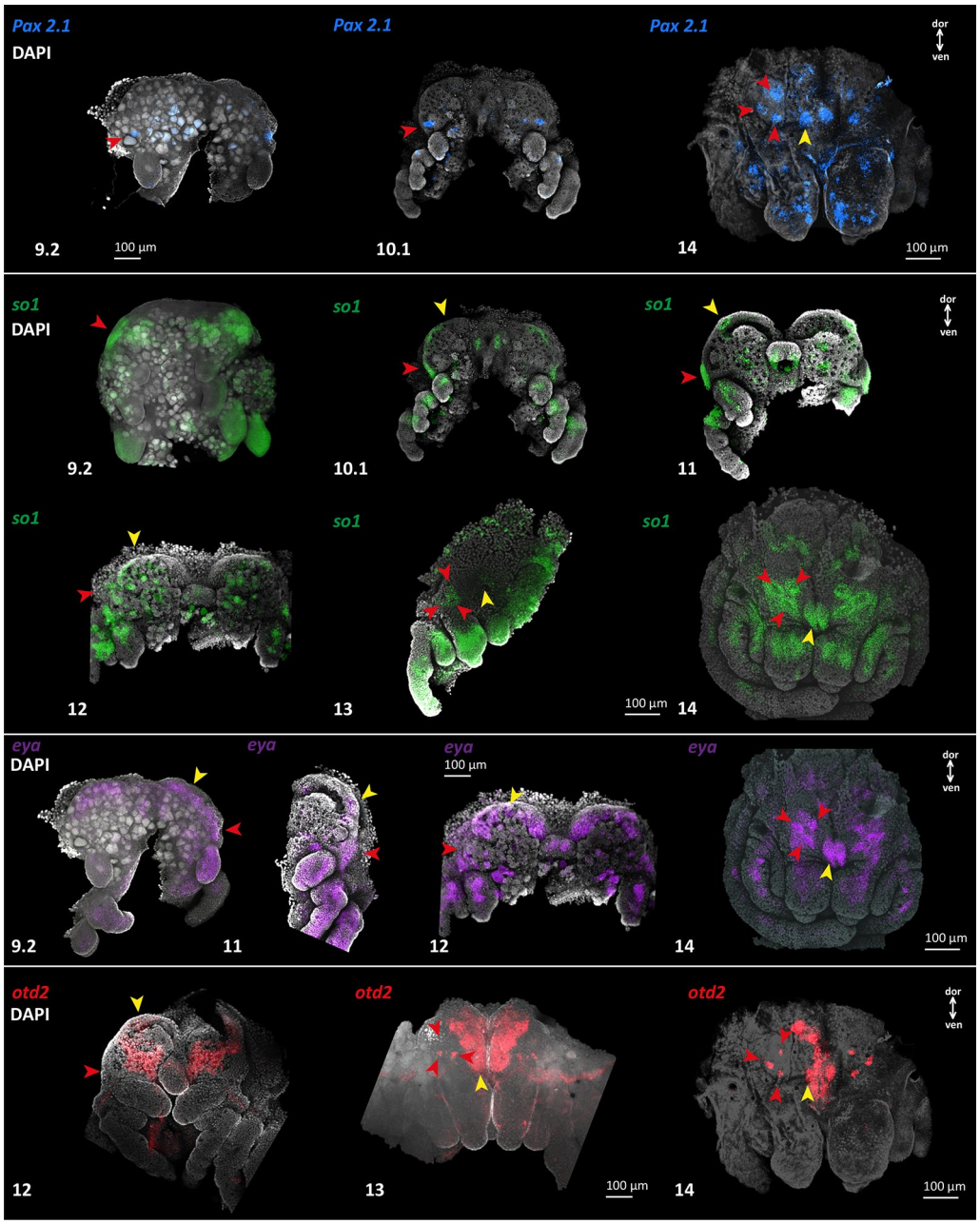

Fig. 6 Retinal determination genes expression in the head region in *T. pagana* embryos on stages 9.2–14. Frontal view of the ocular and cheliceral segments, maximum intensity projections. The colors show the expression of each gene, the embryo is stained with DAPI. Red arrowheads indicate secondary eyes formation, and yellow arrowheads indicate principal eyes formation

expression was observed in all eye types as circular, symmetrical patches (Fig. 6 st. 14, *Pax2.1*). This same condition has previously been reported for Pax2 homologs of a scorpion and a harvestman [11].

sine oculis 1 (*so1*): We observed the expression of *sine oculis 1* (*so1*) at all stages studied in both principal and secondary eyes (Fig. 6, *so1*). At the earliest stage studied, 9.2, the signal is only visible in the secondary eye region as two symmetric patches above the chelicerae on the lateral sides of the precheliceral lobes. At stage 10.1 *so1* is expressed symmetrically in a crescent form in the precheliceral lobes and lateral sides of stomodeum. At stage 11 the same pattern appears with a more concentrated signal in the anterior and lateral furrow regions. At stage 12 there are two pairs of patches in the anterior furrow region and above the chelicera, where the secondary

eyes should form. In stage 13, there are three symmetric round patches in the three forming secondary eyes above the chelicerae and a weaker signal in the median part of the forming brain above the labrum. Finally, at stage 14, there is a strong symmetrical signal in all three secondary eyes above the chelicerae and in the principal eyes above the labrum in oval patches.

eyes absent (eya): We detected the expression of *eyes absent* (*eya*) and found it has a similar expression pattern to *so1*. We also detected *eya* in both principal and secondary eyes (Fig. 6, *eya*). In contrast to *so1* at stage 9.2, *eya* expression is visible in the principal and secondary eye regions as two symmetric crescent patches above the chelicerae on the lateral sides of the precheliceral lobes. Later, at stage 11, there are symmetric patches above the chelicerae in the region of secondary eyes formation and a small oval patch in the median part of the anterior furrow. At stage 12, the same expression pattern is visible for secondary eyes; for the principal eyes, the expression zone expands to all anterior furrows and there is also a symmetric signal in the labral region. Then, in stage 14, the expression pattern is the same as in *so1*: three symmetric round spots in the secondary eyes and one oval in both principal eyes. *so1* expression in stronger at the periphery of the secondary eyes, and *eya* is stronger at the center. This is similar to the expression in the median eyes of *P. opilio* [11].

orthodenticle 2 (*otd2*): We were unable to find a first copy of the *orthodenticle* in the developmental transcriptome. The only copy we found was *otd2*. *otd2* expression was visualized at stages 12, 13, and 14. At stage 12 expression is visible only in the principal eyes as two symmetric patches in the center of precheliceral lobes. At stage 13 it starts to be expressed in the two lower secondary eyes as small symmetric round patches, with expression of two symmetrical elongated patches in the median brain region (including the principal eyes). Finally, at stage 14, *otd2* is expressed in all eyes, as three symmetric round patches in the secondary eyes and as symmetric oval patches in the principal eyes (Fig. 6, *otd2*).

dachshund 1 (dac1): *dachshund 1* (*dac1*) expression was studied at stages 11–14. At stage 11 there are two symmetrical patches at the lateral furrow and a weaker signal at the anterior furrow. There is also a weak symmetrical signal in the middle of the precheliceral lobe and medial subdivision. At stage 12 the expression pattern remains the same as in stage 11: two symmetrical patches above the chelicerae (secondary eyes region), a weak symmetric signal in the middle of the anterior furrow, and three symmetrical triangular patches in the middle of the precheliceral lobe. Stage 13: strong symmetrical signal above the chelicerae and in the lateral parts of the brain and no signal in the principal eyes region. Finally, at stage 14, there is expression above the secondary eyes in two symmetrical crescent patches (Fig. 7).

dachshund 2 (*dac2*): At stage 11, there is expression in the form of two symmetrical oval patches above the chelicerae, in the area of the secondary eyes, as well as small zones in the area of the principal eyes. However, at stage 14, there is expression only in secondary eyes as three symmetrical round patches and no expression in the principal eyes (Fig. 7).

Six3.2:*Six3.2* is expressed only in the principal eyes in early stages and then only in the secondary eyes in later stages. At stage 9.2 there are two symmetrical lines at the top of the precheliceral region. Then, at stage 11, there is symmetrical expression in the anterior furrow and medial subdivision and no signal in the lateral furrow. At stage 14 the expression pattern changes and there is a symmetrical signal in secondary eyes as three round patches, in the labrum region, and no expression in principal eyes.

atonal 1 (ato1):*atonal 1* (*ato1*) expression was studied in three stages 11, 12, and 14. At stage 11 there is no signal in any eye region. At stage 12 there is a bilateral expression domain in the anterior furrow and medial subdivision (principal eyes region) and at stage 14 there is symmetrical *ato1* expression in both secondary and principal eyes in the same manner as *otd2*.

Discussion

1. *Spider embryonic development*

The development of *T. pagana* has more similarities with the development of *C. salei* than with *P. tepidariorum,* consistent with the phylogenetic proximity of *Tegenaria* and *Cupiennius* as members of the RTA clade [21]. The early stages of development in *T. pagana* are quite similar to those of *P. tepidariorum* [25] and *C. salei* [46]. As in *C. salei* and unlike in *P. tepidariorum,* we observe significantly higher nuclear density in the region of the primary thickening; the elevation is likely not a product of additional cell divisions but a product of the change in cellular shape. The lack of a clear germ disc in *T. pagana* is more similar to *C. salei* development. Regarding eye development, we observed the same movement of the secondary eyes as described in *P. tepidariorum* [25]: a 45° rotation in a medial direction so the entire secondary eye complex moves posteriorly. Appendage segmentation appears earlier in *T. pagana* than in *P. tepidariorum* [25] and *C. salei* [46]. The opisthosomal segments become distinct earlier in *T. pagana* but their number grows more slowly than in other studied species. There is less of a size difference between the opisthosomal buds in *T. pagana* and *C. salei* unlike in *P. tepidariorum.* Formation

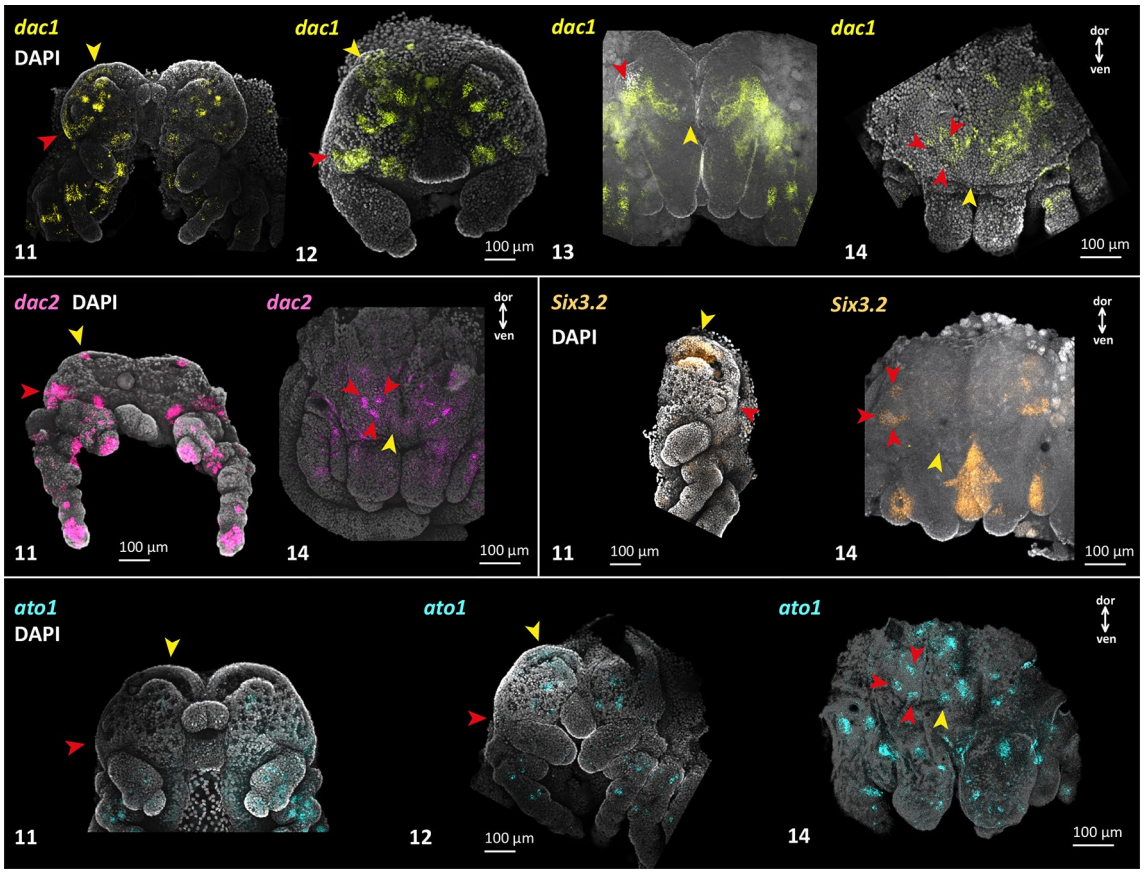

Fig. 7 Retinal determination genes expression in the head region in *T. pagana* embryos on stages 11–14. Frontal view of the ocular and cheliceral segments, maximum intensity projections. The colors show the expression of each gene, the embryo is stained with DAPI. Red arrowheads indicate secondary eyes formation, and yellow arrowheads indicate principal eyes formation

of the respiratory system in *T. pagana* is as difficult to observe; like in *P. tepidariorum*, the development of the book lungs and tubular tracheae is more internalized than in *C. salei.*

As shown by a comparison of the main works on embryonic development [2, 23, 25, 28, 29, 35, 40, 44, 46, 48] with our observations, the embryonic development of spiders is rather conserved. This conservatism is consistent with previous findings on the anatomy of the smallest spiders, showing that even miniaturization does not change the conserved spider anatomy [31]. Nevertheless, we note that there are minor differences in embryogenesis across Entelegynae: the width and degree of development of the ventral sulcus, the presence or absence of a germ disc, a different number of opisthosomal segments at stages 9–10, and the shape of the opisthosomal processes, as well as the duration of development. When it comes to "Haplogynae" and Mygalomorphae, the main difference in embryogenesis is a downturned, tube-shaped opisthosoma posterior the third opisthosomal segment [40, 44], a condition that is plesiomorphic across an array of chelicerate diversity, e.g., mites; ticks; harvestmen; pseudoscorpions; scorpions; [18, 40].

2. Retinal determination gene network in spiders

Our data support previously reported results [17] that there is expression of *Pax2.1* above the chelicerae and lateral to the forming lateral furrow, presumably in the field which later gives rise to the secondary eyes (Fig. 8, blue). It is expressed in *T. pagana* in the same pattern as in *P. tepidariorum* and in the Synspermiata cellar spider *Pholcus phalangioides* (Fuesslin, 1775). However, data on the expression of *Pax2.1* in all eye types at late stages of development contradict the hypothesis of its functional replacement of *Pax6*.

Functional data from a recent study on RDN genes in arachnids showed that *so1* is necessary for patterning all eyes in the spider *P. tepidariorum*, including the principal eyes and secondary eyes [10]. It also seems that the expression pattern of *so1* (Fig. 8, green) and *eya* (Fig. 8, purple) are rather similar in all studied Araneomorphae

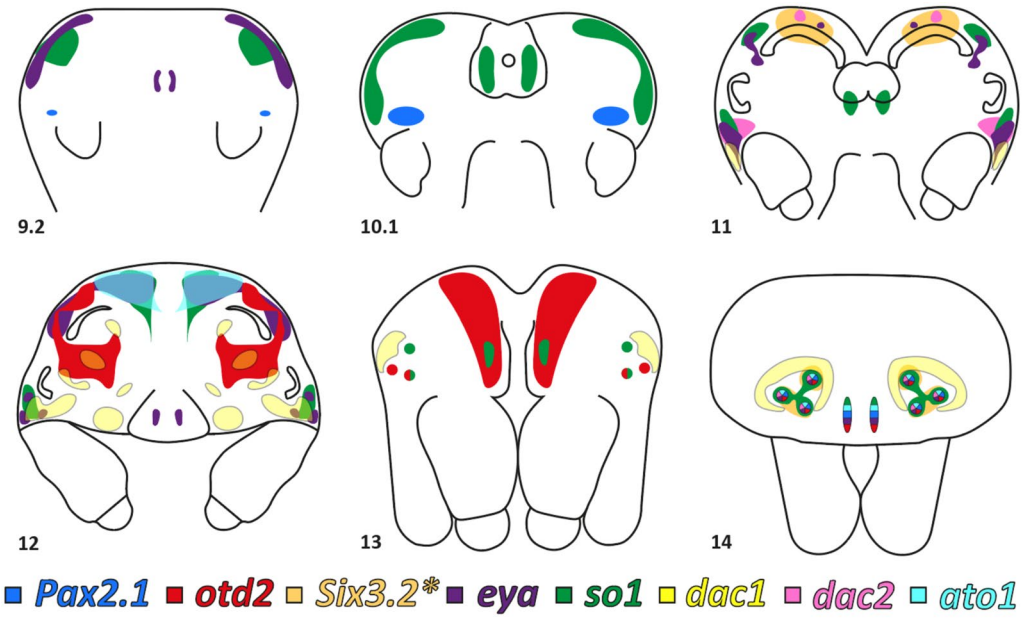

Fig. 8 Schemes of the RDN genes expression patterns in *T. pagana* in different stages

[4, 36, 38]. Moreover, both these genes (*so1* and *eya*) were detected in the principal eye primordia up to stage 10/11 in *Spermophora senoculata* (Dugès, 1836), a spider species that lacks principal eyes [12]. These data suggest a conserved function of these genes in eye formation in spiders.

One of the most interesting results was the *orthodenticle* gene and its paralogs. The absence of *otd1* in the transcriptome likelye reflects the dataset's incompleteness. In contrast to *otd2*, *otd1* is expressed in the opisthosomal limb buds [41]. Therefore, *otd1* is present in another *Tegenaria* species. *Tegenaria pagana otd2* (Fig. 8, red) seems to have almost the same expression patterns as *otd2* in the developing spider brain of all other studied spider species [4], whereas in the eyes, it is either detected only in principal eyes as in *P. tepidariorum*; [12, 39] or exclusively in lateral eyes as in *C. salei* [36]. In *T. pagana otd2* is expressed in both eye types so it is unlikely that this gene is involved in the differentiation of principal and secondary eyes. It is worth noting a slight delay in *otd2* expression in the upper secondary eye (appearing only at stage 14, while in the others, expression appears from stage 13).

As for eye differentiation, *dac* paralogs are involved in determination of the secondary eyes and are not detected in principal eyes in all studied spider species [12, 36, 38]. There are, however, differences; in some cases, expression does not split into distinct domains corresponding to individual eyes, but instead persists as one contiguous domain even after the splitting of the individual eyes [12]. In *T. pagana dac2* (Fig. 8, pink) is expressed in individual eyes and *dac1* (Fig. 8, yellow), even in stage 14, is expressed around the secondary eyes area rather than in the eyes themselves.

As for *Six3.2* (Fig. 8, orange), in previously studied species it is expressed exclusively in secondary eyes or in principal and secondary eyes [4, 37]. In *T. pagana Six3.2* expression was detected first in the principal eye formation zone at stage 12 and later, on stage 14, it was detected as a continuous line in lateral and anterior secondary eyes and as a separate patch in the upper secondary eyes similar to its expression in later stages of *C. salei* development [36]. In *P. tepidariorum* loss of *Six3.1/3.2* function [37] showed no deleterious effect in the anterior median region, suggesting a compensatory effect for two copies.

Unlike in *C. salei* we have observed *ato1* expression (Fig. 8, cyan) not only in early stages in the anterior furrow region, but also in stage 14 as in other spider species [4, 38] as its expression appears in the first photoreceptor cells. At the same time, *ato1* expression in the majority of the studied spiders appears simultaneously in both types of eyes, whereas in *T. pagana,* it is first detected in the principal eyes.

Thus, as in previously studied spider species, a greater number of genes are expressed in the secondary eyes (Fig. 9A), although in early periods of development, some genes can be observed in the primary eyes (Fig. 9B).

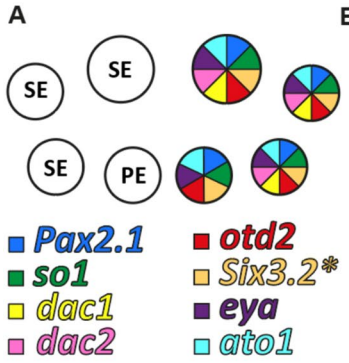

B Principal eyes

Gene	st. 10	st. 11	st. 12	st. 13	st. 14
Pax2.1	–				+
so1	+	+	+	+	+
otd2			+	+	+
Six3.2		+			–
dac1		–	–	–	–
dac2		+			–
eya		+	+		+
ato1		–	–		+

Secondary eyes

Gene	st. 10	st. 11	st. 12	st. 13	st. 14
Pax2.1	+				+
so1	+	+	+	+	+
otd2			–	+	+
Six3.2		–			+
dac1		+	+	+	+
dac2		+			+
eya		+	+		+
ato1		–	–		+

Fig. 9 Combining RDN gene expression data. **A** Scheme of eyes of *T. pagana* with gene expression patterns. PE, principal eyes, SE, secondary eyes. **B** Tables showing presence (+) or absence (–) of gene expression at different stages of embryogenesis of *T. pagana*, blanks—no data

Conclusions

The establishment of protocols for culturing *T. pagana* and studying their embryos provides tools for pursuing comparative study of troglomorphism across the genus *Tegenaria*. The staging system provided here circumvents some of the challenges imposed by species with asynchronous development. Together with genomic resources and approaches for surveying gene expression, we anticipate that *T. pagana* and its troglomorphic congeners may serve as useful models for understanding the evolution of eye loss in arachnids. Future efforts must target the acquisition of comparable embryonic stages of blind *Tegenaria* species, with the goal of surveying RDN genes expression in those taxa.

Methods

Collecting, maintaining spider culture, and copulation

Specimens of *Tegenaria pagana* were collected in Te'omim cave (31°43′37″N 35°01′23″E) in Israel. In total, 27 females, 19 males, and more than 20 juveniles were collected. Each spider was placed in a separate plastic container 15 cm high and 10 cm wide. We poured autoclaved soil and stones into the bottom of the container. The containers were kept in an incubator with a constant humidity of 50% and a temperature of 20–25 °C, without light. For additional moisture, a piece of paper with water was placed at the bottom of the container and was moistened once a week. Every week, each adult spider was given 10–20 fruit flies (*Drosophila melanogaster*), and each spiderling was given one fruit fly at a time, then gave more flies as they grew.

There were 175 copulations in total and 144 of these were successful. One to two days before mating, the spiders were fed. For mating, we waited until the female had built an extensive web in the container, then we carefully removed the male from his container and placed him in the container with the female. We left the pair in the female's container in a thermostat without light for 6–12 h. In rare cases, the male or female killed their partner (males were killed eight times, females two times). Usually, females lay their first egg sac 14–20 days after the first copulation.

After mating, females were checked every day for egg sacs. An egg sac was left with the female for a maximum of 3 days and after which, it was removed and kept in a separate vial, under the same conditions as adults. After the hatching, spiderlings were kept together until they reached an opisthosomal size of approximately 1 to 2 mm. For the study of the embryos, some egg sacs were opened using two forceps, and in general, the eggs simply rolled out of the egg sac separately, with just a few sticking to the silk. Embryos were maintained at 20 °C, reflecting ambient temperature in the species' natural habitat.

Fixation and DAPI staining

Eggs from the egg sacs were carefully transferred to a glass petri dish, dechorionated for 2–3 min in bleach, and then washed 5–7 times with 1X PBS. Embryos were maintained in glass dishes in 1X PBS to develop before fixation. To describe the morphology of *Tegenaria* embryos we stained them with DAPI and examined them using an FV-1200 confocal microscope (Olympus, Japan) and Eclipse 80i fluorescence microscopes (Nikon, Japan) in the Bio-Imaging Unit of The Alexander Silberman Institute of Life Science (The Hebrew University of Jerusalem, Israel).

Embryos were collected and fixed daily (in the period from 12 to 7PM) in 4 ml of 5% formaldehyde in PBS and 4 ml heptane. The solution was gently shaken until embryos were in the phase between heptane and formaldehyde + PBS. Fixation time was 1 h 45 min for stages 1–4 and 8–14, and overnight for stages 4–7. Then, heptane and formaldehyde + PBS were replaced and

embryos were rinsed several times quickly with PBS-T (Tween-20) to stop the fixation. Then, washed 3 times for 5 min each in PBS-T. After washing, the PBS-T was gradually replaced with MeOH in a dehydration series, with 5–10 min between each transition. Once in 100% MeOH, embryos were washed 3 times for 5 min each with 100% MeOH to ensure complete dehydration and then stored at − 20 °C till DAPI staining. DAPI staining was performed for 35 min (2 µL of DAPI in 1 mL PBS-T) then embryos were washed in PBS-T solution for 15 min twice. Slides were prepared using pure glycerol.

Probe synthesis

Description of the developmental transcriptome of *T. pagana* is beyond the scope of this paper and will be provided elsewhere (Propistsova et al. unpublished data). Homologs of the Retinal Determination Network genes were identified in the *T. pagana* developmental transcriptome (Suppl. 2) or the embryos at stage 8 using best reciprocal BLAST (tBLASTn) searches based on query peptide sequences (Suppl. 3) from the GenBank database, multiple sequence alignment, and maximum likelihood inference of the gene tree topologies (Suppl. 4). Probes (Suppl. 5) for HCR were designed using HCR 3.0 Probe Maker [19].

In situ hybridization chain reaction

In situ hybridization was performed according to the Hybridization Chain Reaction (HCR) In Situ Protocol [6]: three PBS + Tween20 washes; permeabilizing 30 min in detergent solution; 30 min in probe hybridization buffer; incubation overnight in probe solution at 37 °C; four washes in probe wash buffer; two washes in 5X SSCT; pre-amplification in amplification buffer; overnight incubation in hairpin solution followed by five washes in 5X SSCT; and 30 min in 1.0 µg/mL DAPI in 50% glycerol solution (in 1X PBS). Images were taken using NIC Zeiss LSM 710 and processed in ImageJ and Photoshop software.

Time-lapse recording

Embryonic development was monitored using time-lapse imaging on a motorized Nikon SMZ25 stereomicroscope for 2–3 weeks for 1 frame per minute (Suppl. 1) and 1 frame per 10 min (Suppl. 6). Double-sided tape was placed at the bottom of the petri dish, embryos were carefully placed on it, and 1X PBS was poured in. The PBS was changed every 2–3 days. PBS was used, because embryos died when reared in halocarbon-700 oil or olive oil.

Staging and timing

For the nomenclature of the embryonic stages, we relied on the embryonic development of *P. tepidariorum* as described by Mittmann and Wolff [25]. The time was calculated based on time-lapse recording, as well as a sequence of photos of various clutches stored in the laboratory from which embryos were taken for fixations. The time indicated is average, since embryos at different stages of development could often be found in the same egg sac and developed asynchronously; even at the same temperature and under the same conditions, the duration of the stages in different clutches could differ twofolds.

Supplementary Information

The online version contains supplementary material available at https://doi.org/10.1186/s13227-025-00238-6.

Supplementary Material 1.
Supplementary Material 2.
Supplementary Material 3.
Supplementary Material 4.
Supplementary Material 5.
Supplementary Material 6.

Acknowledgements

We thank Sharon Warburg, Siddharth Kulkarni, Shlomi Aharon, Zeana Ganem, Hugh G. Steiner, and Yuval Zaltz for their help with collecting material, and Iman Abu Sara for assistance in caring for the embryos. We also thank Benjamin C. Klementz and Kaitlyn Abshire for their help with HCR. In addition, we are grateful to Naomi Melamed-Book, Sarah Swanson, and Gregory Perelman for their support with the confocal microscopes.

Author contributions

EAP collected spiders and embryos, established a colony, designed probes, performed DAPI staining and HCR, analyzed the data, wrote and edited the manuscript; GG collected spiders and embryos, performed a part of the HCR, edited the manuscript; ADC designed the study, edited the manuscript; PPS designed the study, collected spiders and embryos, edited the manuscript, and acquired the funds; EGR designed the study, collected spiders, edited the manuscript and acquired the funds.

Funding

EAP: Doctoral Scholarship for New Immigrants from the Israel Ministry of Absorption. EAP: Prof. Rahamimoff Travel Grant for Young Scientists of the US-Israel Binational Science Foundation no. 3083000024. EGR and PPS: United States National Science Foundation and United States—Israel Bi-national Science Foundation Grant No. 2019823. PPS: National Science Foundation Grant No. IOS-2016141. ADC: Israel Science Foundation Grant No. 570/21.

Availability of data and materials

Original HCR confocal files are available on Zenodo repository, https://doi.org/10.5281/zenodo.13835874 Spiders and egg-sacs were collected under permits from the Israel Nature and Parks Authority to Efrat Gavish-Regev (2018/42037; 2018/41999; 2020/42450; 2021/42815; 2022/43117, 2023-43413).

Declarations

Ethics approval and consent to participate

Not applicable.

Consent for publication
Not applicable.

Competing interests
The authors declare no competing interests.

Author details
[1]The Department of Ecology, Evolution and Behavior, The Hebrew University of Jerusalem, Jerusalem, Israel. [2]The National Natural History Collections, The Hebrew University of Jerusalem, Jerusalem, Israel. [3]Department of Systems Biology, Harvard Medical School, Boston, USA. [4]Department of Pathology, Boston Children's Hospital, Boston, USA. [5]Department of Integrative Biology, University of Wisconsin-Madison, Madison, USA. [6]Zoological Museum, University of Wisconsin-Madison, Madison, WI, USA.

Received: 2 October 2024 Accepted: 20 February 2025
Published: 8 March 2025

References

1. Aharon S, Ballesteros JA, Gainett G, Hawlena D, Sharma PP, Gavish-Regev E. In the land of the blind: exceptional subterranean speciation of cryptic troglobitic spiders of the genus *Tegenaria* (Araneae: Agelenidae) in Israel. Mol Phylogenet Evol. 2023;183:107705.
2. Akiyama-Oda Y, Oda H. Early patterning of the spider embryo: a cluster of mesenchymal cells at the cumulus produces *Dpp* signals received by germ disc epithelial cells. Development. 2003;130:1735–47.
3. Arendt D. Evolution of eyes and photoreceptor cell types. Int J Dev Biol. 2003;47(7–8):563–71.
4. Baudouin-Gonzalez L, Harper A, McGregor AP, Sumner-Rooney L. Regulation of eye determination and regionalization in the spider *Parasteatoda tepidariorum*. Cells. 2022;11:631.
5. Blackburn DC, Conley KW, Plachetzki DC, Kempler K, Battelle B, Brown NL. Isolation and expression of *Pax6* and *atonal* homologues in the American horseshoe crab, *Limulus polyphemus*. Dev Dyn. 2008;237:2209–19. https://doi.org/10.1002/dvdy.21634.
6. Bruce HS, Jerz G, Kelly S, McCarthy J, Pomerantz A, Senevirathne G, et al. Hybridization chain reaction (HCR) in situ protocol. Protocolslo. 2021. https://doi.org/10.17504/protocols.io.bunznvf6.
7. Culver DC. Cave life. Cambridge, London: Harvard University Press; 1982. https://doi.org/10.4159/harvard.9780674330214/html.
8. Foelix RF. Biology of spiders. Insect Syst Evol. 1983;14:16.
9. Friedrich M. Coming into clear sight at last: ancestral and derived events during chelicerate visual system development. BioEssays. 2022;44:2200163. https://doi.org/10.1002/bies.202200163.
10. Gainett G, Ballesteros JA, Kanzler CR, Zehms JT, Zern JM, Aharon S, et al. Systemic paralogy and function of retinal determination network homologs in arachnids. BMC Genom. 2020;21:811. https://doi.org/10.1186/s12864-020-07149-x.
11. Gainett G, Klementz BC, Blaszczyk P, Setton EVW, Murayama GP, Willemart R, et al. Vestigial organs alter fossil placements in an ancient group of terrestrial chelicerates. Curr Biol. 2024;34:1258-1270.e5.
12. Gonzalez LB, Schoenauer A, Harper A, Arif S, Leite DJ, Steinhoff POM, et al. Development and patterning of a highly versatile visual system in spiders. bioRxiv. 2024. https://doi.org/10.1101/2023.12.22.572789.
13. Herman A, Brandvain Y, Weagley J, Jeffery WR, Keene AC, Kono TJY, et al. The role of gene flow in rapid and repeated evolution of cave-related traits in Mexican tetra, *Astyanax mexicanus*. Mol Ecol. 2018;27:4397–416. https://doi.org/10.1111/mec.14877.
14. Hilbrant M, Damen WGM, McGregor AP. Evolutionary crossroads in developmental biology: the spider *Parasteatoda tepidariorum*. Development. 2012;139:2655–62.
15. Howarth FG. High-stress subterranean habitats and evolutionary change in cave-inhabiting arthropods. Am Nat. 1993;142:S65-77. https://doi.org/10.1086/285523.
16. Howarth FG, Moldovan OT. The ecological classification of cave animals and their adaptations. Berlin: Springer; 2018. p. 41–67. https://doi.org/10.1007/978-3-319-98852-8_4.
17. Janeschik M, Schacht MI, Platten F, Turetzek N. It takes two: discovery of spider *Pax2* duplicates indicates prominent role in chelicerate central nervous system, eye, as well as external sense organ precursor formation and diversification after neo- and subfunctionalization. Front Ecol Evol. 2022. https://doi.org/10.3389/fevo.2022.810077/full.
18. Klementz BC, Brenneis G, Hinne IA, Laumer EM, Neu SM, Hareid GM, et al. A novel expression domain of *extradenticle* underlies the evolutionary developmental origin of the chelicerate patella. Mol Biol Evol. 2024. https://doi.org/10.1093/molbev/msae188/7749772.
19. Kuehn E, et al. Segment number threshold determines juvenile onset of germline cluster expansion in Platynereis dumerilii. J Exp Zoology Part B Mol Dev Evol. 2022;338:225–40.
20. Kulkarni S, Wood HM, Hormiga G. Advances in the reconstruction of the spider tree of life: a roadmap for spider systematics and comparative studies. Cladistics. 2023. https://doi.org/10.1111/cla.12557.
21. Kulkarni S, Wood HM, Hormiga G. Phylogenomics illuminates the evolution of orb webs, respiratory systems and the biogeographic history of the world's smallest orb-weaving spiders (Araneae, Araneoidea, Symphytognathoids). Mol Phylogenet Evol. 2023;186:107855.
22. Kumar JP. Retinal determination. In: Cagan RL, Reh TA, editors. Invertebrate and vertebrate eye development. Cambridge: Academic Press; 2010. p. 1–28.
23. Liu Y, Maas A, Waloszek D. Early development of the anterior body region of the grey widow spider *Latrodectus geometricus* Koch, 1841 (Theridiidae, Araneae). Arthropod Struct Dev. 2009;38:401–16.
24. Mammola S, Isaia M. Spiders in caves. Proc R Soc B Biol Sci. 2017;284:20170193. https://doi.org/10.1098/rspb.2017.0193.
25. Mittmann B, Wolff C. Embryonic development and staging of the cobweb spider *Parasteatoda tepidariorum* C. L. Koch, 1841 (syn.: *Achaearanea tepidariorum*; Araneomorphae; Theridiidae). Dev Genes Evol. 2012;222:189–216. https://doi.org/10.1007/s00427-012-0401-0.
26. Morehouse N. Spider vision. Curr Biol. 2020;30:R975–80.
27. Morehouse NI, Buschbeck EK, Zurek DB, Steck M, Porter ML. Molecular evolution of spider vision: new opportunities, familiar players. Biol Bull. 2017;233:21–38. https://doi.org/10.1086/693977.
28. Pechmann M. Embryonic development and secondary axis induction in the Brazilian white knee tarantula *Acanthoscurria geniculata*, C. L. Koch, 1841 (Araneae; Mygalomorphae; Theraphosidae). Dev Genes Evol. 2020;230:75–94. https://doi.org/10.1007/s00427-020-00653-w.
29. Pechmann M, Prpic N-M. Appendage patterning in the South American bird spider *Acanthoscurria geniculata* (Araneae: Mygalomorphae). Dev Genes Evol. 2009;219:189–98. https://doi.org/10.1007/s00427-009-0279-7.
30. Porter ML, Dittmar K, Pérez-Losada M. How Long does evolution of the troglomorphic form take? Estimating divergence times in *Astyanax mexicanus*. Acta Carsol. 2007. https://doi.org/10.3986/ac.v36i1.219.
31. Poulson TL, White WB. The cave environment. Science. 1969;165:971–81. https://doi.org/10.1126/science.165.3897.971.
32. Propistsova EA, Makarova AA, Eskov KY, Polilov AA. Miniaturization does not change conserved spider anatomy, a case study on spider *Rayforstia* (Araneae: Anapidae). Sci Rep. 2023;13:17219.
33. Protas M, Jeffery WR. Evolution and development in cave animals: from fish to crustaceans. Wiley Interdiscip Rev Dev Biol. 2012;1:823–45. https://doi.org/10.1002/wdev.61.
34. Re C, Fišer Ž, Perez J, Tacdol A, Trontelj P, Protas ME. Common genetic basis of eye and pigment loss in two distinct cave populations of the isopod crustacean *Asellus aquaticus*. Integr Comp Biol. 2018;58:421–30.
35. Rempel JG. The embryology of the black widow spider, *Latrodectus mactans* (Fabr.). Can J Zool. 1957;35:35–74. https://doi.org/10.1139/z57-004.
36. Samadi L, Schmid A, Eriksson BJ. Differential expression of retinal determination genes in the principal and secondary eyes of *Cupiennius salei* Keyserling (1877). EvoDevo. 2015;6:16.
37. Schacht MI, Schomburg C, Bucher G. *six3* acts upstream of *foxQ2* in labrum and neural development in the spider *Parasteatoda tepidariorum*. Dev Genes Evol. 2020;230:95.
38. Schomburg C, Turetzek N, Schacht MI, Schneider J, Kirfel P, Prpic N-M, et al. Molecular characterization and embryonic origin of the eyes in the common house spider *Parasteatoda tepidariorum*. EvoDevo. 2015;6:15. https://doi.org/10.1186/s13227-015-0011-9.
39. Schwager EE, Sharma PP, Clarke T, Leite DJ, Wierschin T, Pechmann M, et al. The house spider genome reveals an ancient whole-genome

duplication during arachnid evolution. BMC Biol. 2017;15:62. https://doi.org/10.1186/s12915-017-0399-x.
40. Setton EVW, Hendrixson BE, Sharma PP. Embryogenesis in a Colorado population of *Aphonopelma hentzi* (Girard, 1852) (Araneae: Mygalomorphae: Theraphosidae): establishing a promising system for the study of mygalomorph development. J Arachnol. 2019;47:209.
41. Simonnet F, Célérier ML, Quéinnec E. Orthodenticle and empty spiracles genes are expressed in a segmental pattern in chelicerates. Dev Genes Evol. 2006;216:467–80. https://doi.org/10.1007/s00427-006-0093-4.
42. Stahl BA, Gross JB, Speiser DI, Oakley TH, Patel NH, Gould DB, et al. A transcriptomic analysis of cave, surface, and hybrid isopod crustaceans of the species *Asellus aquaticus*. PLoS ONE. 2015;10: e0140484. https://doi.org/10.1371/journal.pone.0140484.
43. Trajano E, de Carvalho MR. Towards a biologically meaningful classification of subterranean organisms: a critical analysis of the Schiner-Racovitza system from a historical perspective, difficulties of its application and implications for conservation. Subterr Biol. 2017;22:1–26.
44. Turetzek N, Prpic N-M. Observations on germ band development in the cellar spider *Pholcus phalangioides*. Dev Genes Evol. 2016;226:413–22. https://doi.org/10.1007/s00427-016-0562-3.
45. Wang K, Wang J, Liang B, Chang J, Zhu Y, Chen J, et al. Eyeless cave-dwelling *Leptonetela* spiders still rely on light. Sci Adv. 2023;9: eadj0348. https://doi.org/10.1126/sciadv.adj0348.
46. Wolff C, Hilbrant M. The embryonic development of the central American wandering spider *Cupiennius salei*. Front Zool. 2011;8:15. https://doi.org/10.1186/1742-9994-8-15.
47. WSC. World spider catalog version 26. 2025. Natural History Museum Bern. https://wsc.nmbe.ch/. Accessed on 01.03.2025.
48. Yamazaki K, Akiyama-Oda Y, Oda H. Expression patterns of a twist-related gene in embryos of the spider *Achaearanea tepidariorum* reveal divergent aspects of mesoderm development in the fly and spider. Zoolog Sci. 2005;22:177–85. https://doi.org/10.2108/zsj.22.177.

Publisher's Note